Nano Energy 54 (2018) 375–382

Contents lists available at ScienceDirect

Nano Energy

journal homepage: www.elsevier.com/locate/nanoen

Full paper

Towards high performance Li metal batteries: Nanoscale surface modification of 3D metal hosts for pre-stored Li metal anodes

Keegan R. Adair[a], Muhammad Iqbal[a], Changhong Wang[a], Yang Zhao[a], Mohammad Norouzi Banis[a], Ruying Li[a], Li Zhang[b], Rong Yang[b], Shigang Lu[b], Xueliang Sun[a,*]

[a] Department of Mechanical and Materials Engineering, University of Western Ontario, 1151 Richmond St, London, Ontario, Canada N6A 3K7
[b] China Automotive Battery Research Institute Co., Ltd, 5th Floor, No. 43, Mining Building, North Sanhuan Middle Road, Haidian District, Beijing P.C. 100088, China

ARTICLE INFO

Keywords:
Lithium metal battery
Cu-Li alloy
3D Li host
Molten Li infusion
Lithium anode

ABSTRACT

The Li metal anode is an ideal candidate for next-generation batteries due to its ultra-high specific capacity (3860 mAh g^{-1}) and low electrochemical potential (−3.040 V vs. standard hydrogen electrode). However, the large volume fluctuations, side reactions, and dendrite growth are serious problems that need to be solved before Li metal batteries (LMBs) can be commercialized. Herein, we develop a lithiophilic 3D Cu nanowire (3D CuNW) host that can enable molten Li infusion into the structure. Interestingly, the 3D host undergoes a structural transformation upon contact with molten Li and forms Cu-Li alloy crystallites on the surface, leading to the development of an ultra-high performance Li metal anode (3D Li@CuLi). The symmetrical cell performance of the 3D Li@CuLi electrode is found to be among the best reported for carbonate-based electrolytes and can achieve greater than 200 cycles at an ultra-high current density of 10 mA cm^{-2}. Furthermore, full cells coupled with $LiFePO_4$ cathodes show excellent cycling stability at a C-rate of 2 C for over 400 cycles with negligible capacity fade. This work provides a scalable and highly effective approach towards the fabrication of high performance 3D hosts with pre-stored Li metal for next-generation battery systems.

1. Introduction

Since their commercialization in the 1990s, Li-ion batteries (LIBs) have been utilized as energy storage devices for portable electronics and electric vehicles (EVs). However, LIBs have nearly reached their physicochemical energy density limit and have little room for further improvement [1]. In order to meet the demands of future technology, next-generation battery systems will require anode materials with specific capacities that surpass that of the graphite (372 mAh g^{-1}) used in traditional LIBs. As one of the most promising anode candidates for next-generation energy storage systems, Li metal possesses an ultra-high specific capacity (3860 mAh g^{-1}) and low electrochemical potential (− 3.040 V vs. standard hydrogen electrode). [2,3] However, the practical application of Li metal batteries (LMBs) has been hindered by the formation of dendritic lithium, [4–6] unstable solid electrolyte interphases (SEI), [7–9] large volume fluctuations, and short circuits which can lead to catastrophic failure and thermal runaway [10]. Moreover, many of these issues are further aggravated at high current densities and need to be addressed before they can be applied in fast charging EV applications.

Many strategies have been employed to mitigate the risk of dendrite formation, including nanoscale interfacial coatings, [11–14] modification of the electrolyte, [15–17] and the development of 3D hosts or interlayers [18–22]. Several protective coatings have been synthesized by chemical vapour deposition (CVD), atomic layer deposition (ALD), and solution-based methods. Many of these nanoscale thin films are capable of preventing side reactions with electrolyte components and generating homogeneous Li^+ flux that can stabilize the surface of Li metal during cycling. Furthermore, electrolyte components such as SEI stabilizing additives and charge transfer regulating salts have been shown to be effective in minimizing dendrite formation. However, many of these novel techniques are only effective at relatively low current densities and cycling capacities, and need further advancements for application in fast charging battery systems. To achieve improved high-rate performances, 3D hosts have been proposed due their ability to successfully limit the “infinite” volume expansion of Li metal and achieve lower localized current densities that can stabilize the stripping/plating process.

3D structures have garnered significant interest for LMBs due to their low costs, high electrical conductivity and ability to form stable hosts for Li metal. Porous current collectors, 3D skeletons, and nanowire-based structures have been developed through a variety of

* Corresponding author.
E-mail address: xsun9@uwo.ca (X. Sun).

https://doi.org/10.1016/j.nanoen.2018.10.002
Received 8 September 2018; Received in revised form 3 October 2018; Accepted 6 October 2018
Available online 10 October 2018
2211-2855/ © 2018 Published by Elsevier Ltd.

chemical and electrochemical procedures [23–27]. However, many of the reported hosts have relied on the Li source originating from the cathode or depend on electrochemical plating of Li into the 3D structures prior to cell assembly, which makes the process unviable for real application. Even with a Coulombic efficiency of 99%, the Li metal anode would be quickly consumed by side reactions with electrolyte components and retain only 36.6% of its initial Li content after 100 cycles. Therefore, the pre-storing of Li into 3D hosts is required in order to compensate for even the smallest inefficiencies associated with the cycling of Li metal.

Previously, Cui et al. proposed a facile thermal infiltration method in which molten Li is infused into a 3D host [28–30]. By confining Li in a 3D structure, the infinite volume change during cycling could be eliminated. Furthermore, the high surface area provided by 3D structures can further lower the localized current density and enable a more stable plating/stripping process. However, the infusion of molten Li requires a "lithiophilic" surface, which has been primarily fabricated through the use of alloy-type materials such as Si or ZnO [29,31–33]. The coating process can add significant fabrication cost and complexity, as well as potentially lowering the electronic conductivity at the host-Li interface.

Herein, for the first time, we design a lithiophilic 3D Cu-Li alloy host for ultra-high performance Li metal batteries. Through a facile fabrication process, copper nanowires are grown directly on a 3D Cu substrate. The capillary forces of the Cu nanowire structure and reactivity of nanoscale Cu with molten Li enable the infusion of Li into the 3D host. Interestingly, the Cu-Li alloy phase formed on the surface of the Cu skeleton can enable symmetric and full cell cycling performances that are among the best reported to date.

2. Experimental section

2.1. Fabrication of 3D Li@CuLi electrodes

Cu foam (Suzhou Jiashide Metal Foam Co.) of approximately 600 μm thickness was submerged in a mixture of 2 M NaOH(aq) and 0.1 M $(NH_4)_2S_2O_8$ for 15 min to form the 3D $Cu(OH)_2$ nanowire structure. After rinsing with deionized water and drying in a vacuum oven for 12 h, the 3D $Cu(OH)_2$ foam was cut into circular disks using a 3/8 in hole punch. Next, the electrodes were placed in a tube furnace and heated under Ar gas flow to 180 °C and held for 2 h before raising the temperature to 265 °C for 3.5 h with 10% H_2 gas flow. After letting the tube furnace cool to room temperature, the 3D CuNW electrodes were quickly transferred to an Ar-filled glovebox. For the Li infusion process, Li foil (China Energy Lithium Co. LTD) was placed in a stainless steel container and heated to 350 °C. The 3D CuNW electrode was placed into contact with the molten Li where the Li infused into the structure to form the final 3D Li@CuLi electrode. The infusion process typically takes less than 20 s. It should be noted that prolonged exposure to the molten Li can cause further reaction and degradation of the mechanical properties of Cu-based materials, and that the electrodes were removed from the hot plate immediately after the Li infusion process.

2.2. Cathode preparation

Full cells were assembled with a $LiFePO_4$ cathode. The $LiFePO_4$ cathode was prepared using N-Methyl-2-pyrrolidone (NMP) and a 8:1:1 ratio slurry consisting of $LiFePO_4$, acetylene black, and PVDF binder, respectively. The slurry was cast on Al foil and an active mass loading of ~ 7.5 mg cm^{-2} was obtained. The C-rate capacity used for full cell cycling is 161 mAh g^{-1}. Full cells were cycled at a constant current in the voltage range of 2.5–4.2 V.

2.3. Electrochemical measurements

Electrochemical analysis was performed using CR2032 coin-type cells. The coin cells were assembled in an ultra-pure argon filled glove box with 2 layers of polypropylene separator (Celgard 2400). The electrolyte used in this study was 1 M $LiPF_6$ in ethylene carbonate (EC): diethyl carbonate (DEC): dimethyl carbonate (DMC) of 1: 1: 1 vol ratio + 10% fluoroethylene carbonate (FEC). The stripping/plating studies were carried out on Arbin BT-2000 and LAND battery testing systems at room temperature. A constant current was applied to the electrodes during repeated stripping/plating with a 5 min rest period between charge/discharge cycles. Electrochemical impedance spectroscopy (EIS) was also performed on a Bio-Logic multichannel potentiostat 3/Z (VMP3) in the frequency range of 500 MHz to 0.1 Hz.

2.4. Characterization

SEM images were taken using Hitachi 3400 N and Hitachi S4800 Scanning Electron Microscopes at an acceleration voltage of 5 kV. Characterization of Li-containing samples by SEM was conducted by disassembling of cells and rinsing the electrode with dimethyl carbonate (DMC) to remove electrolyte and salts from the surface. To observe the cross-section images of the electrodes, the samples were cut using sharp scissors. The SEM was equipped with an energy dispersive X-ray spectroscopy (EDX) attachment and measurements were undertaken using a working voltage of 20 kV for mapping. Materials were characterized by X-ray diffraction (XRD) using a Bruker D8 Advance machine with Cu Kα radiation. Diffraction data were collected with a 0.01° interval step intervals with an air-sensitive sample holder. The values of the crystal parameters of the new Cu-Li cubic-phase was determined by the d-spacing of the respective reflections. Furthermore, the crystal structures and precise lattice parameters were determined via a two-phase Rietveld refinement method using the RIETAN-FP computer program.

3. Results and discussion

The synthesis of the 3D Li@CuLi electrode follows a facile fabrication process where the intermediate structures are illustrated in Fig. 1**A**. First, a porous 3D Cu foam was submerged in an aqueous solution of $(NH_4)_2S_2O_8$ and NaOH for ~ 15 mins to form copper hydroxide nanowires on the surface (3D $Cu(OH)_2$NW) through a solution mediated process. After rinsing with deionized water and drying in a vacuum oven, the 3D $Cu(OH)_2$NW electrodes were placed in a tube furnace and heated under Ar and H_2 gas flow to reduce the hydroxide nanowires and yield an electrode with an extended 3D Cu nanowire network on the surface (3D CuNW). In the final fabrication step, the 3D CuNW electrode was placed into contact with molten Li which infused into the structure over a period of 1–20 s (Fig. 1**B**), forming a Li composite electrode (3D Li@CuLi). In comparison, the 3D Cu foam structure without nanowires is shown to possess non-wetting behaviour and cannot infuse Li into the 3D host (Fig. 1**C**). The lithiophilic behaviour of the 3D CuNW electrode can be attributed to the surface energy of the nanowires and capillary forces that can enable infusion of molten Li into the host. Furthermore, we find that the thermal infusion process leads to the formation of a new interfacial structure, which will be discussed in the following sections.

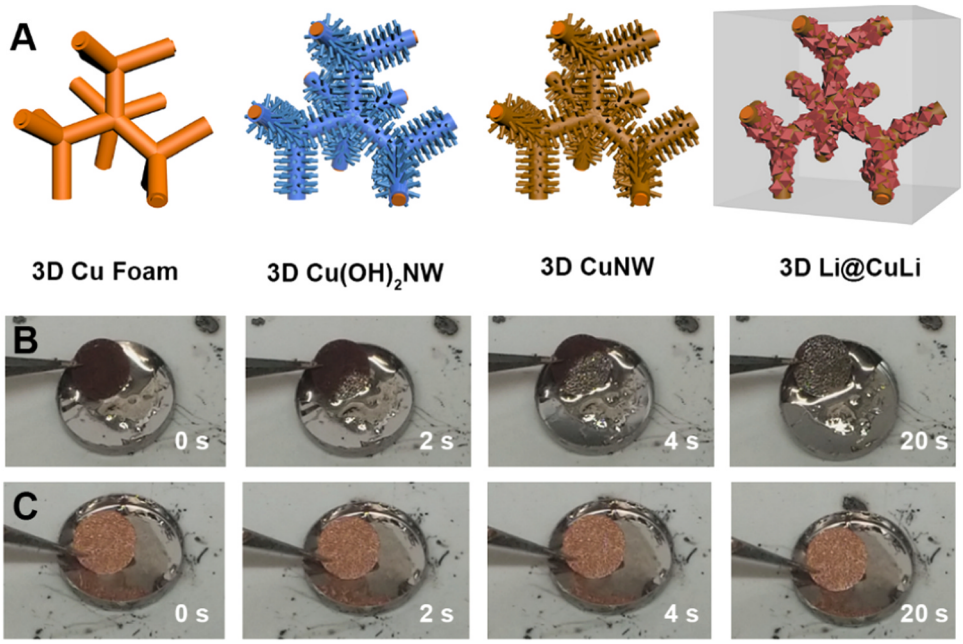

Fig. 1. (A) Schematic diagram of the different stages of electrode fabrication. (B) Molten Li infusion into the 3D CuNW electrode over 20 s and (C) the non-wetting behaviour of the 3D Cu foam.

To study the changes in electrode composition, X-ray diffraction (XRD) was carried out at different stages of the fabrication process (Figs. 2**A and** 2**B**). Upon H_2 reduction and formation of the 3D CuNW electrode, a clean spectrum with the typical Cu peaks was obtained, confirming the complete transformation from the $Cu(OH)_2$ to a Cu nanowire network (Fig. S1). The conversion to a Cu-based structure was further confirmed by energy dispersive X-ray spectroscopy (EDX) mapping, as seen in Fig. S2. However, an interesting phenomenon is observed upon infusion of molten lithium into the structure, as shown by the XRD spectrum of 3D Li@CuLi. In addition to the expected Cu and Li peaks, a new set of peaks appear downshifted to a lower 2θ value from the original Cu positions. To further understand the origins of the new diffraction peaks, we utilized a two-phase Rietveld refinement using the least squares approach. The refined XRD spectrum of the 3D Li@CuLi electrode over an extended range is displayed in Fig. S3 and yields Bragg reflections of a cubic Fm-3 m space group. The new set of peaks downshifted from the Cu metal positions correspond to a lattice parameter of 3.646 Å. Further crystallographic parameters obtained from Reitveld refinement can be found in Table S1. We attribute the new set of peaks to the formation of a secondary Cu-Li phase in which Li has been inserted into the Cu crystal structure, leading to the expansion of the lattice from 3.615 Å to 3.646 Å. The obtained XRD spectra and calculated lattice parameters are in good agreement with the characterizations found by other studies on the formation of Cu-Li alloys with Li content of up to 20 at% [34–36].

Further observation of the 3D structures by SEM reveals significant changes in surface morphology during the different stages of electrode synthesis. Fig. 2**C and D** show arrays of $Cu(OH)_2$ nanowires grown on the surface of 3D Cu foam with high aspect ratios and lengths of approximately 10–15 μm. In addition, some ball-like formations of nanowires are dispersed sparesely on the surface of the host structure. Upon heating in the presence of H_2 and Ar, the $Cu(OH)_2$ nanowires are reduced to Cu and form metallic nanowires on the surface (Figs. 2**E and** 2**F**). In comparison to the $Cu(OH)_2$ nanowire morphology, the Cu nanowires are shrunken and consist of agglomerations of Cu nanoparticles with void spaces formed from the removal of oxygen. Furthermore, molten Li infusion into the host leads to a nearly complete occupation of the void space within the porous structure, as seen in Figs. 2**G and** 2**H**. The filling of the void space between the metal framework leads to a host structure with a maximized energy density (Fig. S4). Interestingly, we can observe particulates dispersed throughout the bulk Li after molten infusion. The particles can be attributed to the formation of Cu-Li alloy crystallites on the exterior surface of the host caused by the reaction of molten Li with Cu, which break free of the host framework during the infusion process. To further study the underlying morphological changes caused by the molten Li infusion, the 3D Li@CuLi electrode was electrochemically stripped of the bulk Li to reveal a new surface consisting of crystallites ranging from 2 to 10 μm in size (Figs. 2**I and** 2**J**). The SEM images of the Cu-Li crystallites are in good agreement with that observed in previous literature. [34,36]

To evaluate the electrochemical performance of the 3D Li@CuLi electrode, symmetrical coin cells were assembled using a carbonate-based electrolyte and cycled at current densities of 3, 5, and 10 mA cm^{-2} with an areal capacity of 1 mAh cm^{-2} (Figs. 3**A-3C**). Figs. 3A and 3B illustrate the electrochemical stability of the 3D Li@CuLi electrode compared to Li foil at high current densities of 3 and 5 mA cm^{-2}. The 3D Li@CuLi electrodes exhibit outstanding electrochemical stability with low overpotentials compared to that of the Li foil. Furthermore, the voltage profiles of the 10th, 50th, and 100th cycles (Fig. S5) reveal that the 3D Li@CuLi can be stabilized after the initial 10 cycles and show limited growth in overpotential during long term cycling. In contrast, the voltage profiles of Li foil are less stable and undergo rapid growth in polarization during cycling due to the continuous SEI growth and consumption of electrolyte. The overpotential of the Li foil cycled at 3 mA cm^{-2} at the 10th, 50th, and 100th cycles are 143 mV, 186 mV, and 445 mV, respectively. Furthermore, cycling of the Li foil symmetrical cells at 5 mA cm^{-2} yields overpotentials of 174 mV, 233 mV, and 549 mV at the 10th, 50th, and 100th cycles, respectively. Moreover, the Li foil voltage profiles gradually form an arcing profile indicative of a tortuous Li^+ transport pathway caused by a thick layer of dead Li. [37] In contrast, the 3D Li@CuLi electrode exhibits low and stable overpotentials of 61 mV and 124 mV at the 100th cycle at 3 and 5 mA cm^{-2}, respectively. When further pushed to an extremely high current density of 10 mA cm^{-2}, the 3D Li@CuLi exhibits outstanding stability and cycle life with minimal overpotential growth for more than 200 cycles. The voltage profile of 3D Li@CuLi fluctuates in the initial cycles due to the stabilization of the SEI and redistribution of Li on the surface. After the initial formation

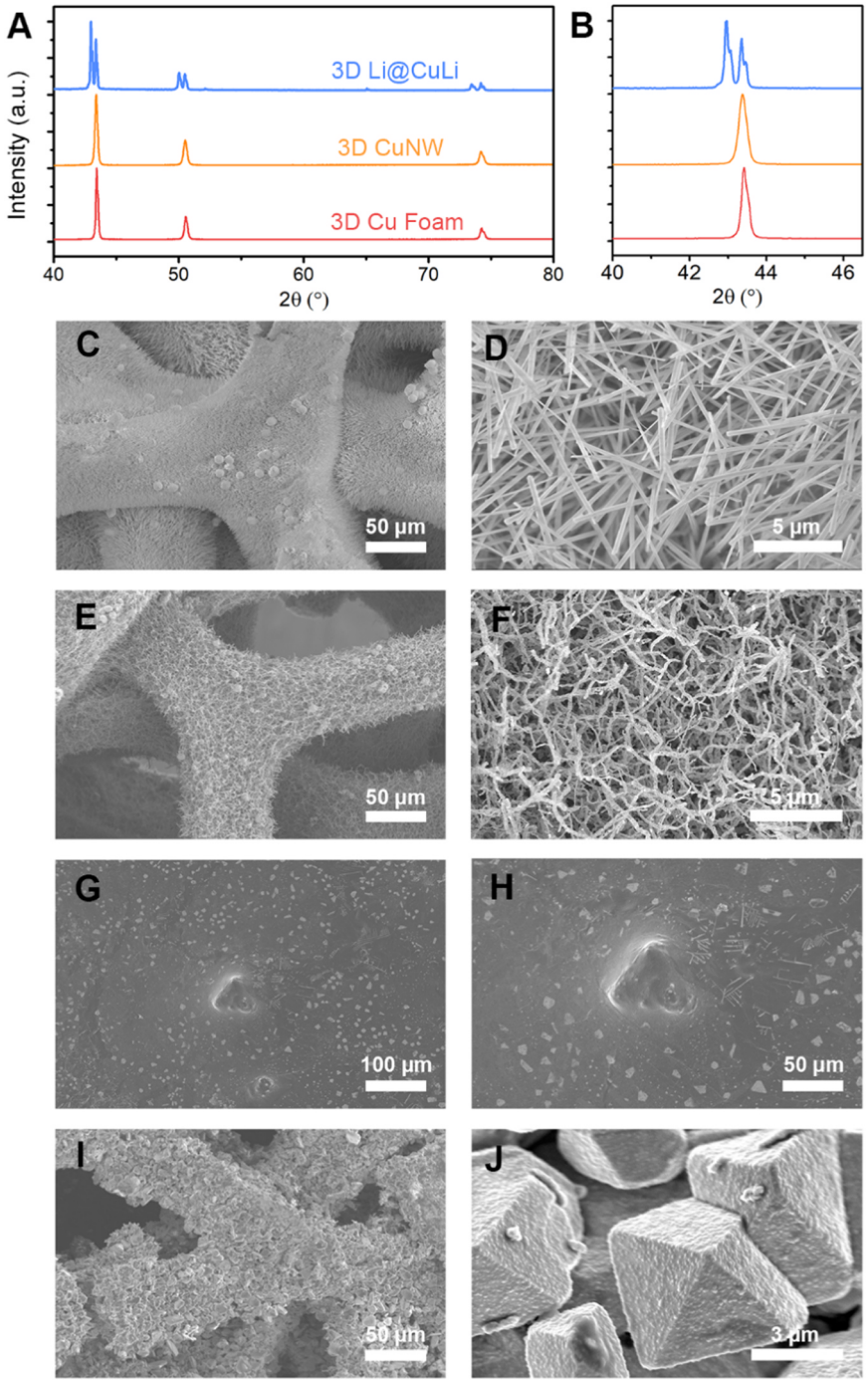

Fig. 2. (A) XRD of the 3D Li@CuLi electrode before and after molten Li infusion and (B) the magnified region between 40° and 46°. (C and D) SEM images of the 3D $Cu(OH)_2$NW electrode. (E and F) SEM images of the 3D CuNW electrode. (G and H) SEM images of the 3D Li@CuLi electrodes after Li infusion. (I and J) SEM images of the 3D Li@CuLi electrodes after electrochemical stripping of the bulk Li content.

cycles, the overpotential can be seen to stabilize at 241 mV and 249 mV at the 50th and 100th cycles (Fig. S5C). In comparison, the Li foil is unable to accommodate the large current density and observes large fluctuations and short-circuiting with overpotentials of 627 mV and 1432 mV at the 50th and 100th cycles, respectively. When cycled at a more modest current density of 1 mA cm^{-2} and capacity of 1 mAh cm^{-2}, the 3D Li@CuLi symmetric cells show overpotentials as low as 40 mV with an ultra-long cycling life of more than 350 cycles with negligible polarization growth (Fig. S6).

As one of the primary advantages of 3D host structures, a large Li reservoir is capable of storing excess Li and can cycle at the large capacities required for commercial application. Complete electrochemical stripping of the bulk Li in the 3D Li@CuLi host yields a gravimetric capacity of 1268 mAh g^{-1} (Fig. S7). This value is similar to the theoretical value calculated in Table S2. Additionally, the 3D Li@CuLi was tested at 1 and 3 mA cm^{-2} with a high areal capacity of 3 mAh cm^{-2} (Fig. S8). The 3D structure is able to successfully accommodate the large cycling capacity and exhibits significantly improved cycling stability compared to the Li foil at both tested current densities, which quickly fails due to the large volume fluctuations and unstable SEI. In terms of symmetric cell cycling in carbonate-based electrolytes, the 3D Li@CuLi anode shows electrochemical performances that are

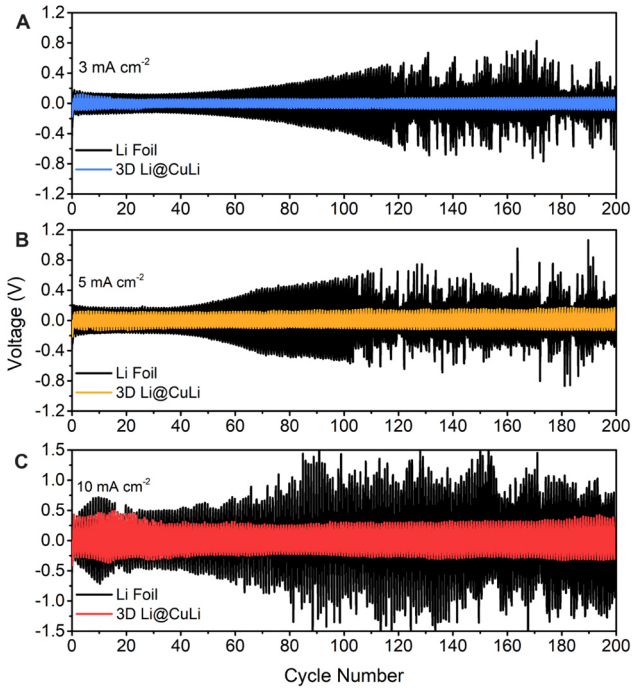

Fig. 3. (A-C) Symmetric cell cycling of the 3D Li@CuLi and Li foil electrodes at current densities of 3, 5, and 10 mA cm^{-2}, respectively.

among the best reported for 3D Li infusion hosts (Table S3).

The reasoning behind the stability and long cycle life of the 3D Li@CuLi electrode was further investigated by SEM images after a complete stripping/plating cycle at different current densities. Fig. S9 compares the surface morphology of Li foil and 3D Li@CuLi at 3, 5, and 10 mA cm^{-2}. It can be seen that even at a current density of 3 mA cm^{-2}, Li deposition on the planar Li foil is non-uniform and results in large aggregates of mossy Li. Upon increasing the current densities to 5 and 10 mA cm^{-2}, more dendritic structures arise and cover the bulk Li surface. In contrast, the 3D Li@CuLi electrode is able to form a stable surface at all tested current densities. At 3 and 5 mA cm^{-2}, Li can be seen to have redeposited preferentially near the host framework and no dendritic structures can be observed. However, when pushed to 10 mA cm^{-2}, the current density appears to be too large for the host framework and results in the deposition of Li throughout the top surface. It is interesting to note that the deposited Li is very dense and uniform, and is likely aided by the Cu-Li crystals dispersed throughout the bulk Li.

To better understand the mechanism behind the improved cycling performance, the 3D Li@CuLi electrodes were cycled to different stages of charge/discharge before disassembly and observation by SEM (Fig. 4). The pristine 3D Li@CuLi electrode shows a relatively smooth surface morphology with Cu-Li crystals dispersed throughout, and areas of the metal foam protruding through the surface (Fig. 4**B**). Upon electrochemical stripping of 1 mAh cm^{-2}, Li can be seen to be removed from the immediate area surrounding the metal framework (Fig. 4**C**). However, further stripping (3 mAh cm^{-2}) leads to an expansion of the void space in the immediate surroundings of the exposed 3D Cu-Li

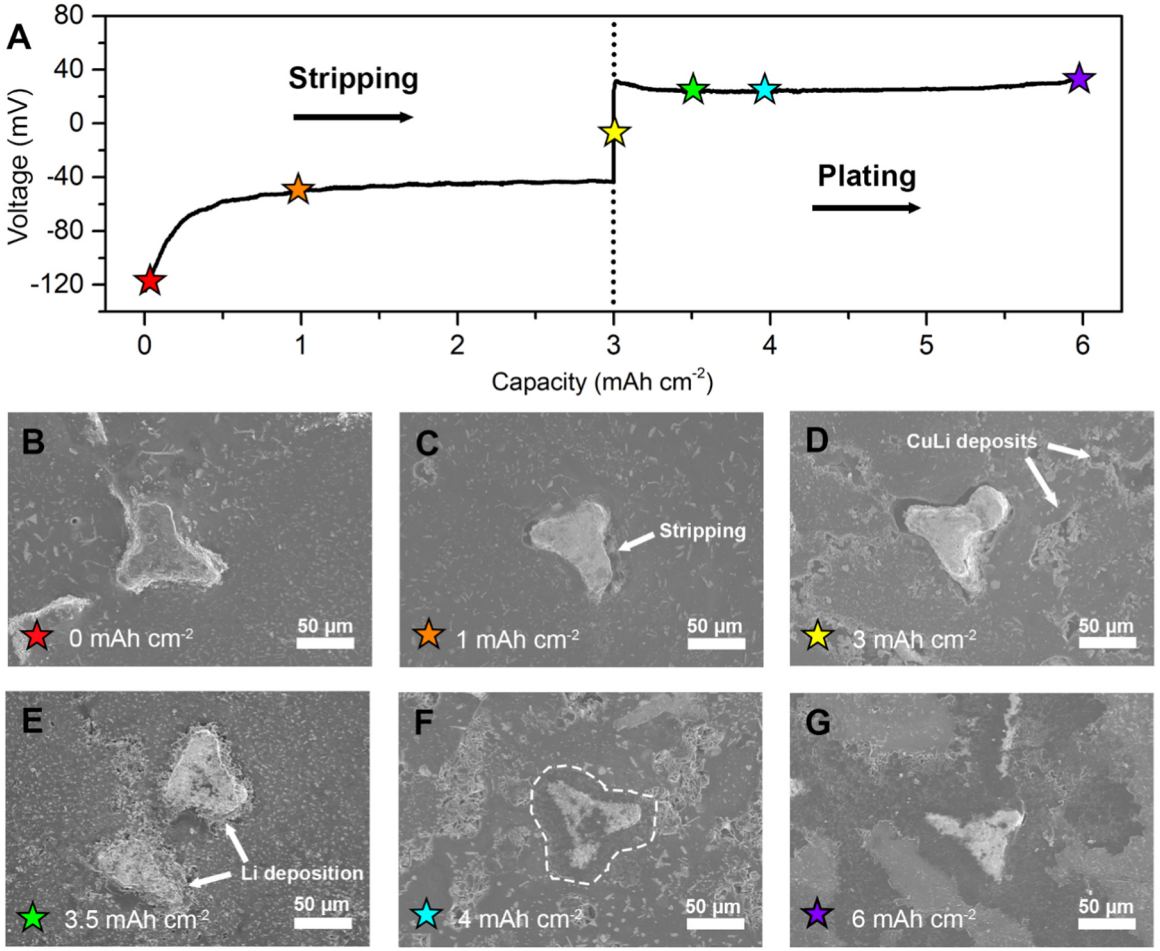

Fig. 4. (A) Representative electrochemical stripping/plating voltage profile of a 3D Li@CuLi electrode at a current density of 1 mA cm^{-2} with a stripping/plating capacity of 3 mAh cm^{-2}. (B-G) SEM images of the 3D Li@CuLi electrode at different stages of the electrochemical stripping/plating cycle.

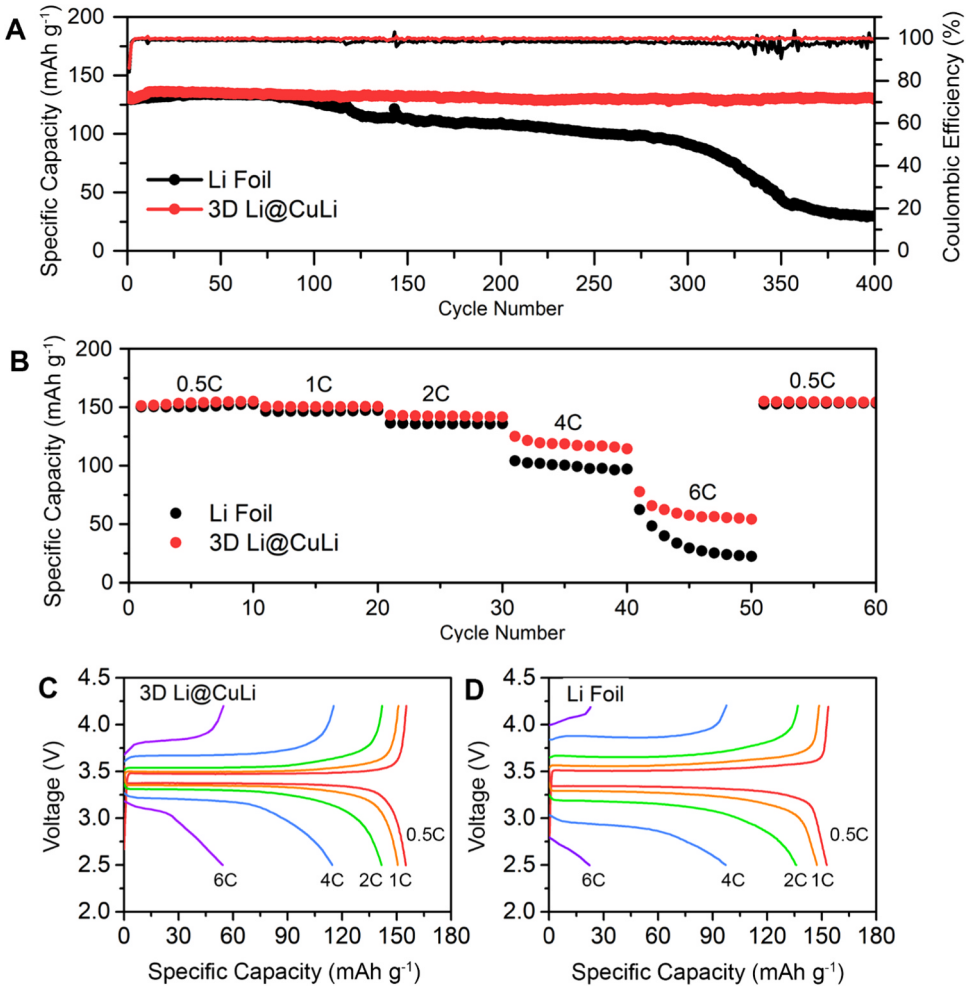

Fig. 5. (A) Electrochemical cycling of full cells with $LiFePO_4$ cathode at a rate of 2 C. (B) The rate performance of full cells containing 3D Li@CuLi anodes compared to Li foil at rates between 0.5C and 6C. (C and D) Voltage profiles of the 3D Li@CuLi and Li foil full cells cycled at rates between 0.5C and 6C.

framework and the onset of pitting of the bulk Li surface (Fig. 4**D**). The pitting regions are observed to contain high concentrations of Cu-Li crystallites, and are likely formed due to complete stripping of the Li in direct contact with the metal framework. To further study the deposition process of Li on the 3D Li@CuLi electrode, Li metal was redeposited and observed at different capacities. Upon plating 0.5 mAh cm^{-2}, SEM reveals that Li preferentially nucleates on the Cu-Li surfaces rather than the top surface of the bulk Li metal (Fig. 4**E**). The direct deposition of Li into the preformed void spaces allows for the confinement of any Li dendrite formation and a more stable deposition process with less volume change. Further deposition leads to complete filling of the voids and a relatively smooth surface morphology (Figs. 4**F and** 4**G**). From these observations, we can attribute the excellent electrochemical performance to the stable nucleation and redeposition of Li into the regions where it was initially stripped. By preferentially depositing on the metal framework and pitted areas with high concentrations of Cu-Li crystallites, the 3D Li@CuLi electrode can avoid inhomogeneous Li nucleation and the formation of dendrites on the surface.

The performance of the 3D Li@CuLi compared to Li foil was further studied in full cells using a $LiFePO_4$ cathode with an active loading of ~ 7.5 mg cm^{-2}. The full cells were cycled at an elevated rate of 2 C for 400 cycles at room temperature. The long term cycling stability displayed in Fig. 5**A** shows that the Li foil and 3D Li@CuLi full cells initially share similar discharge capacities (135 mAh g^{-1}). However, the capacity of the full cell with Li foil begins to fade after the first 100 cycles, followed by a gradual decline until the capacity begins to rapidly roll over and fail at 300 cycles. In comparison, the full cell containing the 3D Li@CuLi exhibits outstanding stability and can cycle more than 400 cycles with negligible capacity fade. Furthermore, EIS measurements of the Li foil and 3D Li@CuLi full cells prior to cycling and after 10 cycles can be seen in Fig. S10. In the initial state, the impedance associated with SEI and charge transfer of the 3D Li@CuLi cell is less than half of that of the Li foil. After 10 cycles at 2 C, the SEI can be seen to stabilize leading to a further decrease in cell impedance. The low impedance can be attributed to the 3D structure of the Li@CuLi electrode which can help stabilize the Li plating process and SEI formation through lowering of the localized current densities.

In addition, the rate capabilities of the Li electrodes were testing in full cells with the $LiFePO_4$ cathodes. Fig. 5**B** illustrates the discharge capacities for cells containing Li foil and 3D Li@CuLi cycled at 0.5 C, 1 C, 2 C, 4 C, and 6 C. While the discharge capacity is similar between the Li electrodes at lower C-rates, the difference in performance becomes apparent when pushed to higher C-rates of 4 C and 6 C. The voltage profiles of the 3D Li@CuLi (Fig. 5**C**) and Li foil (Fig. 5**D**) full cells at the corresponding C-rates further exhibit the advantages of the 3D host structure. The 2D planar structure of Li foil is able to maintain similar discharge capacities and voltage hysteresis to the 3D Li@CuLi host at low current densities, however, when pushed to higher C-rates, is unable to accommodate the high Li^+ flux and leads to large voltage polarizations. The discharge capacities of the Li foil full cell are approximately 153, 147, 135, 97, and 22 mAh g^{-1} at the C-rates of 0.5 C, 1 C, 2 C, 4 C, and 6 C, respectively. On the other hand, the 3D Li@CuLi structure can sustain high current densities while minimizing the

voltage hysteresis and maintaining high discharge capacities. In comparison, the discharge capacities of the 3D Li@CuLi full cell are 155, 151, 142, 115, and 55 mAh g^{-1} at 0.5 C, 1 C, 2 C, 4 C, and 6 C, respectively.

4. Conclusions

Herein, we have designed a high performance lithiophilic Cu-based 3D host for Li metal batteries. The Cu nanowire morphology has been shown to enable molten Li infusion into the 3D host structure, which subsequently reacts with the nano Cu surface to produce a Cu-Li alloy. The 3D Li@CuLi host has been shown to be capable of sustaining ultra-high current densities during electrochemical tests and possesses some of the best high-rate cycling performances among the previously reported literature. Furthermore, the mechanism of electrochemical plating/stripping has been revealed and it was found that the Cu-Li crystals can serve as nucleation centers and help stabilize the electrodeposition process at high current densities. Lastly, full cell batteries assembled with $LiFePO_4$ cathodes show outstanding cycling stability and lifetime, achieving over 400 cycles at a rate of 2 C with negligible capacity decay. We believe that this work will shed insight into the design of high performance Li metal batteries and serve as the basis for future work on 3D Cu hosts with pre-stored Li.

Acknowledgments

This research was supported by the Natural Science and Engineering Research Council of Canada (NSERC), the Canada Research Chair Program (CRC), the Canada Foundation for Innovation (CFI), the China Automotive Battery Research Institute-Western University Joint Laboratory, and Western University.

Author contribution

K.R.A and X.S. conceived this work; K.R.A. designed and fabricated experiments. K.R.A., M.I., C.W., and M.N.B. performed characterization of the electrodes; All authors contributed to the data analysis and preparation of the manuscript.

Declaration of interests

The authors declare no competing interests.

Appendix A. Supporting information

Supplementary data associated with this article can be found in the online version at doi:10.1016/j.nanoen.2018.10.002

References

[1] J.W. Choi, D. Aurbach, Nat. Rev. Mater. 1 (2016) 16013.
[2] Z. Tu, P. Nath, Y. Lu, M.D. Tikekar, L.A. Archer, Acc. Chem. Res. 48 (2015) 2947–2956.
[3] X.B. Cheng, R. Zhang, C.Z. Zhao, F. Wei, J.G. Zhang, Q. Zhang, Adv. Sci. 3 (2016) 1500213.
[4] P. Bai, J. Li, F.R. Brushett, M.Z. Bazant, Energy Environ. Sci. 9 (2016) 3221–3229.
[5] K.N. Wood, E. Kazyak, A.F. Chadwick, K.H. Chen, J.G. Zhang, K. Thornton, N.P. Dasgupta, ACS Cent. Sci. 2 (2016) 790–801.
[6] X. Wang, W. Zeng, L. Hong, W. Xu, H. Yang, F. Wang, H. Duan, M. Tang, H. Jiang, Nat. Energy 3 (2018) 227–235.
[7] Z. Liu, Y. Qi, Y.X. Lin, L. Chen, P. Lu, L.Q. Chen, J. Electrochem. Soc. 163 (2016) A592–A598.
[8] X.-Q. Zhang, X.-B. Cheng, X. Chen, C. Yan, Q. Zhang, Adv. Funct. Mater. 27 (2017) 1605989.
[9] D. Lu, Y. Shao, T. Lozano, W.D. Bennett, G.L. Graff, B. Polzin, J. Zhang, M.H. Engelhard, N.T. Saenz, W.A. Henderson, P. Bhattacharya, J. Liu, J. Xiao, Adv. Energy Mater. 5 (2015) 1400993.
[10] D. Lin, Y. Liu, Y. Cui, Nat. Nanotechnol. 12 (2017) 194–206.
[11] J. Zhao, L. Liao, F. Shi, T. Lei, G. Chen, A. Pei, J. Sun, K. Yan, G. Zhou, J. Xie, C. Liu, Y. Li, Z. Liang, Z. Bao, Y. Cui, J. Am. Chem. Soc. 139 (2017) 11550–11558.
[12] Y. Zhao, L.V. Goncharova, Q. Sun, X. Li, A. Lushington, B. Wang, R. Li, F. Dai, M. Cai, X. Sun, Small Methods (2018) 1700417.
[13] N.W. Li, Y.X. Yin, C.P. Yang, Y.G. Guo, Adv. Mater. 28 (2016) 1853–1858.
[14] L. Wang, L. Zhang, Q. Wang, W. Li, B. Wu, W. Jia, Y. Wang, J. Li, H. Li, Energy Storage Mater. 10 (2018) 16–23.
[15] A. Basile, A.I. Bhatt, A.P. O'Mullane, Nat. Commun. 7 (2016) 11794.
[16] F. Ding, W. Xu, G.L. Graff, J. Zhang, M.L. Sushko, X. Chen, Y. Shao, M.H. Engelhard, Z. Nie, J. Xiao, X. Liu, P.V. Sushko, J. Liu, J.G. Zhang, J. Am. Chem. Soc. 135 (2013) 4450–4456.
[17] J. Qian, W.A. Henderson, W. Xu, P. Bhattacharya, M. Engelhard, O. Borodin, J.G. Zhang, Nat. Commun. 6 (2015) 6362.
[18] Y. Zhao, Q. Sun, X. Li, C. Wang, Y. Sun, K.R. Adair, R. Li, X. Sun, Nano Energy 43 (2018) 368–375.
[19] H. Wang, D. Lin, Y. Liu, Y. Cui, Sci. Adv. 3 (2017) e1701301.
[20] D. Lin, J. Zhao, J. Sun, H. Yao, Y. Liu, K. Yan, Y. Cui, Proc. Natl. Acad. Sci. USA 114 (2017) 4613–4618.
[21] H. Lee, J. Song, Y.J. Kim, J.K. Park, H.T. Kim, Sci. Rep. 6 (2016) 30830.
[22] S.-S. Chi, Y. Liu, W.-L. Song, L.-Z. Fan, Q. Zhang, Adv. Funct. Mater. 27 (2017) 1700348.
[23] C.P. Yang, Y.X. Yin, S.F. Zhang, N.W. Li, Y.G. Guo, Nat. Commun. 6 (2015) 8058.
[24] Q. Li, S. Zhu, Y. Lu, Adv. Funct. Mater. 27 (2017) 1606422.
[25] H. Zhao, D. Lei, Y.-B. He, Y. Yuan, Q. Yun, B. Ni, W. Lv, B. Li, Q.-H. Yang, F. Kang, J. Lu, Adv. Energy Mater. (2018) 1800266.
[26] L.L. Lu, J. Ge, J.N. Yang, S.M. Chen, H.B. Yao, F. Zhou, S.H. Yu, Nano Lett. 16 (2016) 4431–4437.
[27] P. Zou, Y. Wang, S.W. Chiang, X. Wang, F. Kang, C. Yang, Nat. Commun. 9 (2018) 464.
[28] Y. Liu, D. Lin, Z. Liang, J. Zhao, K. Yan, Y. Cui, Nat. Commun. 7 (2016) 10992.
[29] Z. Liang, D. Lin, J. Zhao, Z. Lu, Y. Liu, C. Liu, Y. Lu, H. Wang, K. Yan, X. Tao, Y. Cui, Proc. Natl. Acad. Sci. USA 113 (2016) 2862–2867.
[30] D. Lin, Y. Liu, Z. Liang, H.W. Lee, J. Sun, H. Wang, K. Yan, J. Xie, Y. Cui, Nat. Nanotechnol. 11 (2016) 626–632.
[31] Y. Zhang, W. Luo, C. Wang, Y. Li, C. Chen, J. Song, J. Dai, E. Hitz, S. Xu, C. Yang, Y. Wang, L. Hu, Proc. Natl. Acad. Sci. USA 114 (2017) 3584–3589.
[32] L. Wang, X. Zhu, Y. Guan, J. Zhang, F. Ai, W. Zhang, Y. Xiang, S. Vijayan, G. Li, Y. Huang, G. Cao, Y. Yang, H. Zhang, Energy Storage Mater. 11 (2018) 191–196.
[33] C. Yang, L. Zhang, W. Luo, B. Liu, Y. Li, S. Xu, T. Hamann, D. McOwen, J. Dai, W. Luo, Y. Gong, E. Wachsman, L. Hu, Proc. Natl. Acad. Sci. USA 115 (2018) 3770–3775.
[34] C.F. Old, P. Trevena, Metal. Sci. 15 (2013) 281–286.
[35] O.A. Lambri, J.I. Pérez-Landazábal, L.M. Salvatierra, V. Recarte, C.E. Bortolotto, O. Herrero, R.E. Bolmaro, A. Peñaloza, C.H. Wörner, Mater. Lett. 59 (2005) 349–354.
[36] A. Peñaloza, M. Ortiz, C.H. Wörner, J. Mater. Sci. Lett. 14 (1995) 511–513.
[37] K.-H. Chen, K.N. Wood, E. Kazyak, W.S. LePage, A.L. Davis, A.J. Sanchez, N.P. Dasgupta, J. Mater. Chem. A 5 (2017) 11671–11681.

Keegan Adair received his B.Sc. in chemistry from the University of British Columbia in 2016. He is currently a Ph.D. candidate in Prof. Xueliang (Andy) Sun's Nanomaterials and Energy Group at the University of Western Ontario, Canada. Keegan has previously worked on battery technology at companies such as E-One Moli Energy and General Motors. His research interests include the design of nanomaterials for lithium metal batteries and nanoscale interfacial coatings for battery applications.

Dr. Muhammad Iqbal is a Postdoctoral research associate at Prof. Xueliang (Andy) Sun's Nanomaterial and Energy Group at the University of Western Ontario Canada. He received his PhD in 2013 from the Department of Electronic Chemistry, Tokyo Institute of Technology, Japan, and after that, he worked as a research associate at the Department of Chemical Science and Engineering, School of Materials and Chemical Technology, Tokyo Institute of Technology, Japan. His primary research interests include catholytes and electrolytes for all-solid-state Li-ion batteries.

Changhong Wang is currently a Ph.D. candidate in Prof. Xueliang (Andy) Sun's Group at the University of Western Ontario, Canada. He got his B.S. in applied chemistry from University of Science and Technology of Anhui in 2011 and obtained his M.S. degree in materials engineering from University of Science and Technology of China in 2014. After graduation, he also served as a research assistant in Singapore University of Technology and Design from 2014 to 2016. Currently, his research interests include solid-state sulfide electrolytes, all-solid-state LIBs and Li-S batteries, and memristors.

Yang Zhao is currently a Ph.D. candidate in Prof. Xueliang (Andy) Sun's Group at the University of Western Ontario, Canada. He received his B.S. degree and M.S. degree in Chemical Engineering and Technology from Northwestern Polytechnical University (Xi'an, China) in 2011 and 2014, respectively. His current research interests focus on atomic/molecular layer deposition in the application of lithium/sodium ion batteries and all-solid-state batteries.

Dr. Mohammad Norouzi Banis is research engineer in Prof. Xueliang (Andy) Sun's group at University of Western Ontario, Canada. He received his Ph.D. degree in 2013 in Materials Science and Engineering from Western University, on the study of nanostructured low temperature fuel cells and application of x-ray absorption spectroscopy in energy related systems. His current research interests include study of metal ion, metal air and nanocatalysts via in-situ synchrotron based techniques.

Ruying Li is a research engineer at Prof. Xueliang (Andy) Sun's Nanomaterial and Energy Group at the University of Western Ontario, Canada. She received her master in Material Chemistry under the direction of Prof. George Thompson in 1999 at University of Manchester, UK, followed by work as a research assistant under the direction of Prof. Keith Mitchell at the University of British Columbia and under the direction of Prof. Jean-Pol Dodelet at l'Institut national de la recherché Scientifique (INRS), Canada. Her current research interests are associated with synthesis and characterization of nanomaterials for electrochemical energy storage and conversion.

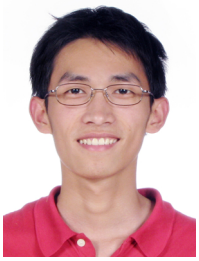

Dr. Li Zhang is currently a senior scientist of China Automotive Battery Research Institute Co., Ltd., Beijing, China. He received his Ph.D. degree in Electrochemistry from University of Science & Technology Beijing, China in 2009. He has more than 10 years of power sources experience with expertise in battery materials as well as electrode design. Currently, his research interests include solid-state electrolytes, all-solid-state Li-air, and lithium batteries.

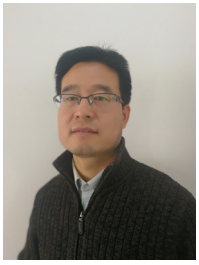

Dr. Rong Yang received his Ph.D. degree in inorganic chemistry from Peking University in 2011. He is currently a senior engineer in China Automotive Battery Research Institute. His research interests are focused on cathode materials for lithium-ion batteries, solid-state lithium ion conductors, and solid-state lithium-ion batteries.

Dr. Shigang Lu is Vice president of China Automotive Battery Research Institute Co., Ltd. He has the responsibility for technology innovations in the area of automotive battery application. He has extensive experience in many energy research areas including fuel cells, and lithium-ion batteries. Dr. Lu received her Ph.D. degree in Chemistry from Moscow State University in 1993. He has extensive experience in novel material processing techniques for automotive battery applications. His current research interests include new energy electrochemistry, lithium-ion battery and related materials, solid-state battery and related materials.

Prof. Xueliang (Andy) Sun is a Canada Research Chair in Development of Nanomaterials for Clean Energy, Fellow of the Royal Society of Canada and Canadian Academy of Engineering and Full Professor at the University of Western Ontario, Canada. Dr. Sun received his Ph.D. in materials chemistry in 1999 from the University of Manchester, UK, which he followed up by working as a postdoctoral fellow at the University of British Columbia, Canada and as a Research Associate at L'Institut National de la Recherche Scientifique (INRS), Canada. His current research interests are focused on advanced materials for electrochemical energy storage and conversion, including electrocatalysis in fuel cells and electrodes in lithium-ion batteries and metal-air batteries.